# Long-Wavelength Collective Excitations in Ferromagnetic Insulators. I. Strong Coupling of Acoustic Modes to Spin Wave Modes

R. C. LeCraw and T. Kasuya*
*Bell Telephone Laboratories, Murray Hill, New Jersey*
(Received 19 September 1962)

Investigations have been made of long-wavelength collective lattice vibrations and long-wavelength spin wave modes in ferromagnetic insulators such as the rare-earth iron garnets. These materials have many different sites for the rare earth ions and generally have unquenched orbital moments. In this paper both theoretical and experimental work are reported with the main consideration being strong coupling effects between acoustic and spin wave modes. The strong coupling produces a field dependence of the resonant frequency and acoustic $Q$ of long-wavelength acoustic modes in saturated (i.e., single domain) samples. The sample shapes employed are spheres and thin disks. Satisfactory agreement is obtained between theory and experiment concerning the field dependences, rare earth concentration dependences, and correlation of acoustic effects with spin resonance quantities, such as linewidth. Also from these results values are obtained of the cubic magnetoelastic coupling constants $B_1$ and $B_2$ for terbium and europium iron garnets.

## I. INTRODUCTION

In these papers we consider long-wavelength collective excitations in ferromagnetic insulators in which there are a number of inequivalent sites for the magnetic ions. We will consider here mainly the rare-earth iron garnets, but actually the treatment is more general and can apply to most ferromagnetic insulators.

In Paper I, we consider interactions between long-wavelength acoustic lattice modes and similarly long-wavelength spin wave modes with an applied dc magnetic field such that the sample is magnetically saturated, that is, a single domain. Until recently the study of elastic properties of ferromagnets has been primarily concerned with effects caused by changes in the domain structure due to an applied dc field, the "$\Delta E$" effect.[1] Also reported are anomalies in the elastic properties due to an applied field which occur near the Curie point, caused by the "paraprocess."[2] No clear, quantitative observations have yet been reported of changes in the elastic properties, as the magnitude of the applied field is varied, in single domain samples well below the Curie point.[3] We report here theory and observations in which both the resonant frequency and relaxation time of ferromagnetic acoustic resonators depend strongly on the magnitude of the applied dc magnetic field well above saturation and well below the Curie point.

## II. MODEL AND EQUATION OF MOTION

For special acoustic lattice modes and acoustic spin wave modes, the Hamiltonian is expanded:

$$\mathcal{H}=\mathcal{H}_0+\tfrac{1}{2}\sum K_\nu\partial^2/\partial\Delta_\nu^2+\sum V_\nu\Delta_\nu+\sum V_pS_p +\tfrac{1}{2}\sum V_{\nu\mu}\Delta_\nu\Delta_\mu+\tfrac{1}{2}\sum V_{\nu p}\Delta_\nu S_p+\tfrac{1}{2}\sum V_{pq}S_pS_q, \quad (1)$$

where $\Delta_\nu$ is a collective lattice vibration mode and $S_p$ a collective spin-wave mode with $x$ and $y$ components. We assume approximately that the commutation relation $[S_{xk},S_{yk}]=i$ exists, where $k$ refers to the class of the mode, or in infinite media to the usual wave vector. In finite media $S_p$ depends on the shape of the sample, such as the Walker modes. The same situation exists for $\Delta_\nu$ also. Hereafter, we represent both $\Delta_\nu$ and $S_p$ by $\Delta_\xi$

The first term of Eq. (1) concerns the so called individual modes and the second term concerns the kinetic term of the collective lattice vibrations. The parameters $K_\nu$, $K_\xi$, and $V_{\xi\eta}$ are obtained, for example, by the Tomonaga method.[4] Among the many possible collective modes, we consider here only special modes with a given "wave vector," or, as seen in Appendix I, an acoustic and an optical lattice vibration together with an acoustic spin-wave mode with $x$ and $y$ components. Generally speaking, however, in a sample of finite dimensions, a free lattice vibration couples to every free spin-wave mode. In such cases, we adopt a forced spin-wave mode which has the same configuration as the lattice vibration under consideration. Because we are considering only long-wavelength lattice vibrations, the exchange effect is not important. In this paper it is unnecessary to specify $V_\xi$, etc., in more detail. More detailed discussions based on a definite model will be given in paper II.

At first, we should treat $\mathcal{H}_0$. However, $\mathcal{H}_0$ is so complicated that it is impossible to treat rigorously. Therefore, as a first approximation we assume three independent modes of the system, namely, thermal phonons, thermal spin waves of the $Fe^{3+}$ lattice, and single ion energy levels of the rare-earth $4f$ electrons. Of course these modes interact with each other and thus have finite life times. Among these we consider here only the effects of the rare-earth energy levels and treat Eq. (1) in the usual adiabatic approximation. This means that since the motions of the collective modes are sufficiently slow, the state of the $4f$ level is

* On leave of absence from the Institute for Solid State Physics, University of Tokyo, Tokyo, Japan.

[1] For a review of this effect, see R. M. Bozorth, *Ferromagnetism* (D. Van Nostrand Company, Inc., Princeton, New Jersey, 1951), pp. 684–712.

[2] K. P. Belov, G. I. Kataev, and R. Z. Levitin, Soviet Phys.—JETP **10**, 670 (1960).

[3] We exclude here such small effects as volume magnetostriction.

[4] S. Tomonaga, Progr. Theoret. Phys. (Kyoto) **13**, 467 (1955).

given corresponding to the instantaneous distortion of the collective coordinates. The effects of nonadiabatic terms and also terms due to other magnons and phonons will be given in subsequent papers.

Due to the collective modes the rare-earth energy levels change as follows:

$$\mathcal{E}_n = \mathcal{E}_n{}^0 + \sum \mathcal{E}_n{}^{\xi}\Delta_{\xi} + \tfrac{1}{2}\sum \mathcal{E}_n{}^{\xi\eta}\Delta_{\xi}\Delta_{\eta}, \tag{2}$$

where $n$ means the special energy level of a rare-earth ion located at the lattice position $R_n$. Assuming substantial separation of the energy levels, $\mathcal{E}_n{}^{\xi}$ and $\mathcal{E}_n{}^{\xi\eta}$ are calculated by the usual perturbation method. As $\Delta_{\xi}$ changes with time, the occupation number $N_n$ also changes. It is solved by the usual Boltzmann equation,

$$dN_n/dt = (dN_n/dt)_{\text{collision}}, \tag{3}$$

where the right side is due to the nondiagonal terms of $\mathcal{H}_0$. We now assume that small driving forces are applied which vary as $\cos\omega t$ and a steady-state condition exists. Then $\Delta_{\xi}$ can be represented by a linear combination of $\cos\omega t$ and $\sin\omega t$ terms and the solution may be written as

$$N_n(t) = N_n{}^0 + \sum_{\xi}[N_n{}^{\xi 0} + N_n{}^{\xi 1}F(t)]\Delta_{\xi}(t), \tag{4}$$

where $N_n{}^0$ is the thermal equilibrium value corresponding to $\mathcal{E}_n{}^0$, namely, no collective mode distortion. If the collision term in Eq. (3) is zero, then $N_n(t)$ is constant with time. The second term of Eq. (4) is due to the rearrangement of the occupation number by collision processes corresponding to the change of $\mathcal{E}_n$, the second term of Eq. (2). $N_n{}^{\xi 0}$ is the in-phase term and corresponds to the frequency shift of the collective modes. $N_n{}^{\xi 1}$ is the out of phase term and corresponds mainly to the damping of the collective modes, $F(t) = (1/\omega)(d/dt)$.

An essential characteristic of our model is that there are nonvanishing contributions to both $\mathcal{E}_n{}^{\nu}$ and $\mathcal{E}_n{}^{p}$. Otherwise, the second term in Eq. (4) disappears. [See Eqs. (16) and (17).] We consider this in more detail: Suppose that the main interaction between the rare-earth ions and $Fe^{3+}$ ions is the usual isotropic exchange interaction. Then it is clear that $\mathcal{E}_n{}^{p}$ is proportional to $\langle n|S_{pR}|n\rangle$, where $S_{pR}$ is the $p$ component of the spin operator of a rare-earth ion at a position $R$. If there are only unique sites for the rare-earth ions, then it must be zero, because we assume that the $z$ direction is chosen in the direction of the magnetization which lies in a symmetry direction. In our model there are many rare-earth sites, and for each of these sites there is a finite value of $\langle n|S_{pR}|n\rangle$, etc., but when averaged over different sites it cancels out and vanishes. Of course the rare-earth garnets and many other materials satisfy the above condition.

The equations of motion for the collective modes are obtained as follows:

$$(\pm)\hbar(dS_p/dt) = F_q + f_q\cos\omega t, \tag{5}$$

$$-(\hbar^2/K_{\nu})(d^2\Delta_{\nu}/dt^2) = F_{\nu} + f_{\nu}\cos\omega t, \tag{6}$$

where the $(\pm)$ corresponds to $(x,y)$ and

$$F_{\xi} = \sum_{\eta}[A_{\xi\eta} + a_{\xi\eta}F(t)]\Delta_{\eta}, \tag{7}$$

$$A_{\xi\eta} = \sum_{n}(N_n{}^0\mathcal{E}_n{}^{\xi\eta} + N_n{}^{\eta 0}\mathcal{E}_n{}^{\xi}) + A_{\xi\eta}{}^0, \tag{8}$$

$$a_{\xi\eta} = \sum_{n} N_n{}^{\eta 1}\mathcal{E}_n{}^{\xi}, \tag{9}$$

where $A_{\xi\eta}{}^0$ is the contribution from other than rare earth $4f$ levels. The first term of Eq. (8), which represents the terms due to rare-earth $4f$ levels, is referred to as $A_{\xi\eta}{}'$ hereafter. With the assumption that the damping terms are sufficiently small, the solutions are obtained as follows (see Appendix I): For the spin-wave modes, assuming the acoustic vibration frequency is much less than the Zeeman frequency and the optical magnetoelastic effect is small,

$$\hbar\omega = (A_{xx}A_{yy})^{1/2}. \tag{10}$$

Or, assuming that the main term is the Zeeman energy of the $Fe^{3+}$ spins,

$$\hbar\Delta\omega \equiv \hbar(\omega - \omega_0) = \tfrac{1}{2}(A_{xx}{}' + A_{yy}{}'), \tag{11}$$

and for the damping term, assuming further that the $x$ and $y$ directions are equivalent and magnetoelastic effects are small,

$$\hbar/\tau_s \equiv g\mu\Delta H = 2a_{pp}, \tag{12}$$

where $\omega_0$ is the Zeeman frequency, namely, $g_{Fo}\mu H_0/\hbar$ in a spherical sample, where $H_0$ is the applied dc magnetic field, and $\Delta H$ is the usual ferromagnetic resonance linewidth (full width). The quantity $\tau_s$ defined by this relation is not necessarily the same as the free-decay spin wave lifetime, $\tau_s{}^0$, because in the present case $A_{\xi\eta}$ is strongly dependent on frequency. Only in the case where the frequency dependence of $A_{\xi\eta}$ is negligible, then $\tau_s$ and $\tau_s{}^0$ are equal. The expression for $\tau_s{}^0$ is, in the present case, much more complicated than Eq. (12). (See Appendix I.) For the acoustic vibration modes, we obtain

$$\Delta\omega/\omega = (1/2A_{\nu\nu}{}^0)[A_{\nu\nu}{}' - \sum_{p}(A_{\nu p}A_{p\nu}/A_{pp})], \tag{13}$$

$$\frac{1}{\omega\tau_a} \equiv \frac{1}{Q} = \frac{1}{A_{\nu\nu}{}^0}\left[a_{\nu\nu} + \sum_{p}\frac{A_{\nu p}A_{p\nu}}{A_{pp}{}^2}a_{pp} - \sum_{p}\frac{2A_{\nu p}a_{\nu p}}{A_{pp}}\right], \tag{14}$$

where $\Delta\omega$ is the deviation of the frequency from that in the absence of rare-earth $4f$ level effects, and $\tau_a$ is the relaxation time of the energy of the freely decaying acoustic mode. Note that because we consider here a low-frequency acoustic mode, the frequency dependence of $A_{\xi\eta}{}^0$ is negligible.

For the simplest case, the collision term of Eq. (3) is written using a single relaxation time as

$$dN_n/dt = -(N_n - N_n{}^{\text{eq}})/\tau, \tag{15}$$

where $N_n^{eq}$ is the thermal equilibrium value corresponding to the instantaneous distortion due to the collective modes. Then the following results are obtained easily:

$$N_n{}^{\xi 0}=\frac{1}{1+(\omega\tau)^2}\sum_m \frac{\partial N_n{}^0}{\partial \mathcal{E}_m{}^0}\mathcal{E}_m{}^\xi, \tag{16}$$

$$N_n{}^{\xi 1}=\frac{-\omega\tau}{1+(\omega\tau)^2}\sum_m \frac{\partial N_n{}^0}{\partial \mathcal{E}_m{}^0}\mathcal{E}_m{}^\xi. \tag{17}$$

And then

$$a_{\xi\eta}=\frac{\omega\tau}{1+(\omega\tau)^2}\frac{N_R}{\kappa T}[\langle\langle n|V_\xi|n\rangle\langle n|V_\eta|n\rangle\rangle_0 - \langle V_\xi\rangle_0\langle V_\eta\rangle_0]_{\rm av}, \tag{18}$$

$$A_{\xi\eta}{}'=N_R\Big[\langle V_{\xi\eta}\rangle_0-\tfrac{1}{2}\sum_n\sum_m\frac{N_n{}^0-N_m{}^0}{\mathcal{E}_m{}^0-\mathcal{E}_n{}^0} \times\{\langle n|V_\xi|m\rangle\langle m|V_\eta|n\rangle+\langle n|V_\eta|m\rangle\langle m|V_\xi|n\rangle\} +\frac{1}{\kappa T}\langle V_\xi\rangle_0\langle V_\eta\rangle_0+\omega\tau a_{\xi\eta}\Big]_{\rm av}, \tag{19}$$

where $N_R$ is the number of rare-earth ions, and

$$\langle V\rangle_0=\sum_n N_n{}^0\langle n|V|n\rangle \tag{20}$$

refers to the thermal average on a site and $[\ ]_{\rm av}$ refers to the average over all different sites. In the second term of Eq. (19) the diagonal term means

$$\lim_{n\to m}\frac{(N_n{}^0-N_m{}^0)}{(\mathcal{E}_m{}^0-\mathcal{E}_n{}^0)}=\frac{N_n{}^0}{\kappa T}. \tag{21}$$

## III. COMPARISON WITH ACOUSTIC EXPERIMENTS

### A. Field Dependence of $\omega$ and $Q^{-1}$

We shall now consider a comparison of the theory with low-frequency ($\sim$1 Mc/sec) acoustic experiments. In Eqs. (13) and (14) the first terms represent the direct interaction between the acoustic distortion and the rare-earth ions and are relatively independent of the applied magnetic field. This is because usually the exchange field is much larger than the applied field. The second terms of Eqs. (13) and (14) are due to the strong coupling of an acoustic lattice mode and a spin-wave mode via the rare-earth $4f$ levels. A characteristic feature of these terms is a strong field dependence because, as the wavelength is very large, the forced spin-wave distortion is inversely proportional to the effective field on the $Fe^{3+}$ spins. Thus, the field dependence of $A_{\xi\eta}$, etc. (except $A_{pp}$), is negligible, and the main field dependence comes from $A_{pp}$. It is written as

$$A_{pp}=g\mu(H_0+H_a), \tag{22}$$

where $g$ is an effective $g$ factor, $H_0$ is the applied dc field, and $H_a$ is an effective anisotropy field including a uniform shift term. Except at very low temperatures, $H_a$ is sufficiently small so that the second terms in Eqs. (13) and (14) exhibit large dependences on the applied field $H_0$. Thus, the field dependence of $\Delta\omega/\omega$ is nearly proportional to $(H_0+H_a)^{-1}$. For $Q^{-1}$ there are two terms, one proportional to $(H_0+H_a)^{-1}$ and another proportional to $(H_0+H_a)^{-2}$. The first term, however, may be considerably smaller than the second term in heavily doped materials, except at very low temperatures and strong magnetic fields. For example, in terbium iron garnet (TbIG) at room temperature, where the present experiments were done, the first term is probably two orders of magnitude smaller than the second. Thus, we may expect that

$$1/Q_H=(1/Q_{\rm obs}-1/Q_\infty)\propto 1/(H_0+H_a)^2, \tag{23}$$

where the subscript $H$ refers to the field-dependent part of $Q$ and the subscripts obs and $\infty$ refer to the observed $Q$ and the $Q$ at infinite applied field, respectively.

In Figs. 1 and 2, we see plots of $\nu=\omega/2\pi$ and $Q_H$ vs $(H_0+H_a)$ obtained at room temperature on single-crystal spheres of TbIG. Figures 3 and 4 show similar plots for YbIG at 78°K. The technique used to obtain these data is essentially the same as outlined previously,[5] except that instead of a continuous wave (cw) method utilizing orthogonal input and output coils, a pulsed scheme is used employing a single coil together with a number of coaxial mercury switches. (See Fig. 5.) After a steady state has been reached, the switches are used to (1) switch the coil from the generator to the receiver, (2) turn off the driving generator, and (3)

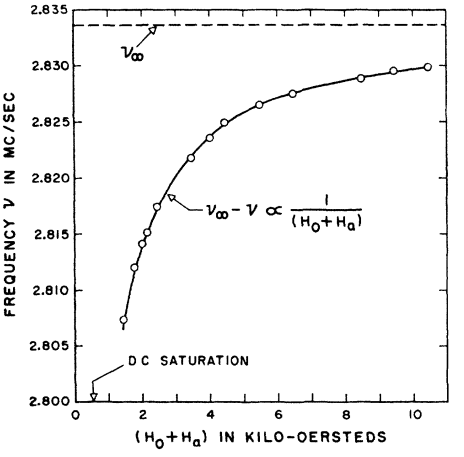


FIG. 1. Resonant frequency vs $(H_0+H_a)$ for a 0.088-in. sphere of TbIG at 298°K for the $T_{11}$ pure shear mode. The circles are the data. The solid theoretical curve has been fitted at 10.45 and 5.45 kOe, yielding $\nu_\infty$ as shown and $H_a=450$ Oe. The applied dc field $H_0$, is along the [111] axis.

[5] R. C. LeCraw, E. G. Spencer, and E. I. Gordon, Phys. Rev. Letters **6**, 620 (1961).

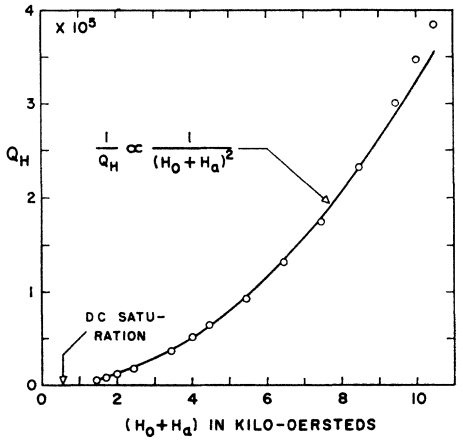


FIG. 2. $Q_H$ vs $(H_0+H_a)$ for TbIG at 298°K, with the same sphere, mode, and dc field direction as in Fig. 1. The solid theoretical curve has been fitted at 8.45 and 4.0 kOe. The same $H_a$ was used as in Fig. 1. In this material, $Q_\infty$ is so large that $Q_H \cong Q_{obs}$, hence this figure is very nearly the same as a plot of the actual observed $Q$ vs $(H_0+H_a)$. See Eq. (23).

turn on the superheterodyne receiver to observe the free decay of the sphere. The sphere rests loosely on the bottom of the evacuated quartz tube. The applied dc field is horizontal, and the applied rf field is approximately vertical.

The acoustic mode observed for the data in Figs. 1–4 is a pure shear mode designated[6] $T_{11}$ with all particle motion lying in planes perpendicular to the mode axis, which is not necessarily parallel to the dc field. Since initially the spheres are free to rotate, the dc field is along an easy axis, [111]. The acoustic motion consists of an inner sphere and an outer shell rotating in opposite directions about the mode axis. Both the driving and detecting processes of this higher order mode are rather complicated and will not be considered further here. However, this mode is one of the few that can be identified unambiguously by its resonant frequency, since there are no other modes particularly close-by in frequency. As is the case for YIG, it appears that TbIG at room temperature and YbIG at 78°K are approximately elastically isotropic in the limit of large applied magnetic fields (though not quite to the degree of YIG). The resonant frequency for the above mode as well as many other modes of an isotropic sphere are given by Lamb.[7]

It is seen that the data for $(\nu_\infty-\nu)$ on both materials are good fits to $(H_0+H_a)^{-1}$ with $H_a=450$ Oe for TbIG and 450 Oe for YbIG. The $\nu_\infty$ corresponds to $(H_0+H_a)$ equal infinity. Also the data for $Q_H^{-1}$ in both materials are good fits to $(H_0+H_a)^{-2}$ using the same values of $H_a$.

[6] The notation here is the authors' and will be described in detail in a separate paper. The first subscript refers to the angular dependence of the displacement, and the second subscript refers to the radial boundary condition and is the root of the appropriate Bessel function.

[7] H. Lamb, London Math. Soc. Proc. 13 (1882). See also, A. E. H. Love, *A Treatise on the Mathematical Theory of Elasticity* (Dover Publications, Inc., New York, 1927), 4th ed.

Because of the complexity of the calculations on spheres we have not evaluated the constants of proportionality to obtain, for example, the magnetoelastic coupling constants. This we do later for disks.

### B. Relation between Acoustic and Linewidth Measurements

Next, it is of interest to examine the ratio of $Q_H^{-1}$ to $\Delta\omega/\omega$. This ratio has a strong correlation with the resonance linewidth because $a_{pp}$ involves the usual spin resonance line width. Considering the frequency difference between the microwave and acoustic resonances, the concentration differences, and also assuming that $a_{xx}=a_{yy}$ and $A_{xx}=A_{yy}$, we obtain from Eqs. (12), (13), (14), (18), and (22)

$$\frac{Q_H^{-1}}{(\Delta\omega_a/\omega_a)_H}=2\left[\frac{a_{pp}}{A_{pp}}\right]_a = \frac{g_r(\Delta H)}{g_a(H_0+H_a)}\frac{\omega_a}{\omega_r}\frac{c_a}{c_r}\left[\frac{1+(\omega_r\tau)^2}{1+(\omega_a\tau)^2}\right], \quad (24)$$

where the subscripts $a$ and $r$ (used only in this section to separate the two frequencies) refer to acoustic and spin resonance, respectively. If both the resonance and acoustic measurement are done with the same sample and at the same frequency, then the last term of Eq. (24) is simply $\Delta H/(H_0+H_a)$. Usually, however, the conditions are different. Note that in heavily doped samples, $g$ and $\Delta H$ depend complicatedly on the rare-earth concentration, $c$, but the product $g\Delta H$ is proportional to $c$ ($c$ being the fraction of yttrium ions replaced with rare-earth ions). In high-temperature approximation, which means that the temperature is higher than the energy separation of the lowest $J$ configuration,

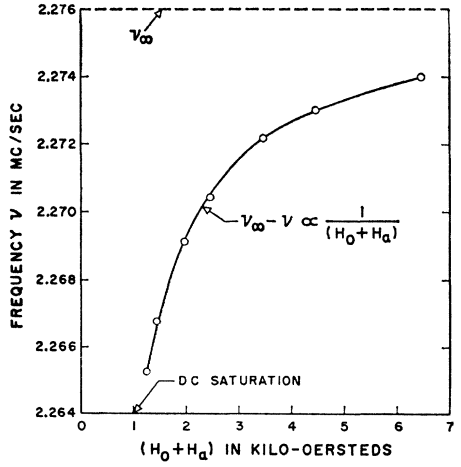


FIG. 3. Resonant frequency vs $(H_0+H_a)$ for a 0.107-in. sphere of YbIG at 78°K for the $T_{11}$ pure shear mode. The circles are the data. The solid theoretical curve has been fitted at 6.45 and 3.45 kOe, yielding $\nu_\infty$ as shown and $H_a=450$ Oe. $H_0$ is along the [111] axis.

but smaller than the energy separation between the lowest and next excited $J$ configuration, then

$$g_{r,a}=2M_{\rm tot}/M_{\rm Fe}, \tag{25}$$

where $M_{\rm tot}$ is the total magnetization and $M_{\rm Fe}$ is the net magnetization of the iron lattice. Usually resonance experiments are done on dilute rare-earth samples, and then $g_r$ is 2. A more detailed discussion of Eqs. (24) and (25) will be given in paper II.

We should like to compare Eq. (24) with experiment for TbIG at room temperature and $\omega_a\sim10^7$ sec$^{-1}$ and $\omega_r\sim10^{11}$ sec$^{-1}$. Here $(\omega_a\tau)^2\ll1$ and $(\omega_r\tau)^2\ll1$ and $g_a\cong2/7$. $M_{\rm tot}$ in Eq. (25) was measured at room temperature on a large sphere of TbIG and found to be approximately 20 G.[8] The linewidth at room temperature was measured at 15.3 kMc/sec and 300°K along a [111] axis of a single-crystal sphere of $(Y_{0.8}Tb_{0.2})_3Fe_5O_{12}$ yielding $\Delta H=4100$ Oe.[9] This is in satisfactory agreement with linear extrapolations from the work of Dillon[10] on much lower percentage dopings of terbium. Thus, using $(H_0+H_a)=4000$ Oe, $\omega_a/2\pi=2.8336$ Mc/sec, $\omega_r/2\pi=15.3$ kMc/sec, $c_a=1$, $c_r=0.2$, and $g_r=2$, we obtain $6.65\times10^{-3}$ for the right side of Eq. (24). From Figs. 1 and 2, the left side of Eq. (24) at the same value of $(H_0+H_a)$ is $5.65\times10^{-3}$, in relatively good agreement.

The same comparison between acoustic and linewidth measurements has been made for YbIG at 78°K, using the data of Teale, Pearson, and Hight[11] and again the agreement is good. Here $(\omega_r\tau)^2$ in Eq. (24) cannot be neglected.

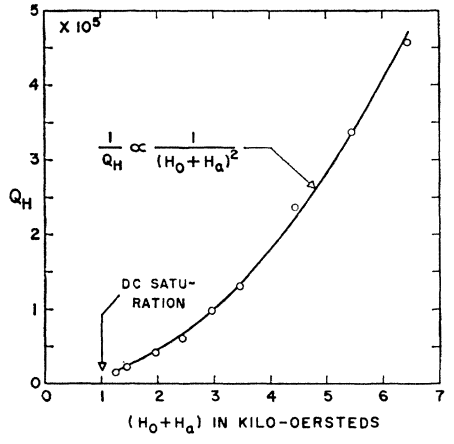


FIG. 4. $Q_H$ vs $(H_0+H_a)$ for YbIG at 78°K, with the same sphere, mode, and dc field direction as in Fig. 3. The solid theoretical curve has been fitted at 5.45 and 2.95 kOe. The same $H_a$ as in Fig. 3 was used.

[8] This measurement was kindly made by R. C. Sherwood of Bell Telephone Laboratories.

[9] This measurement was kindly made by W. H. Hewitt, Jr., and separately by E. M. Gyorgy of Bell Telephone Laboratories.

[10] J. F. Dillon, Jr., and J. W. Nielsen, Phys. Rev. Letters 3, 30 (1959).

[11] R. W. Teale, R. F. Pearson, and M. J. Hight, Suppl. J. Appl. Phys. 32, 150S (1961).

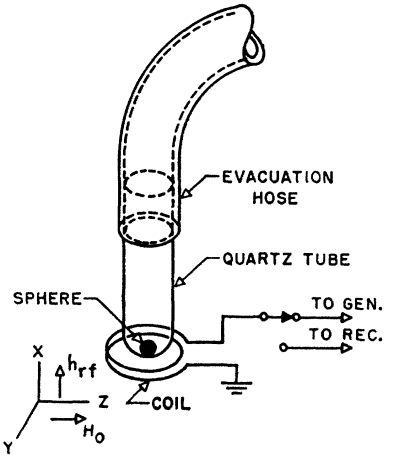


FIG. 5. Schematic diagram of driving and detecting method for spheres. The single-pole double-throw switch permits the same coil to be used for both driving and detecting the acoustic motion. The switch is activated after steady state is reached, and the free decay is then observed in the receiver.

### C. Rare-Earth Concentration Dependence

The rare-earth concentration dependence of the acoustic properties was studied in the following samples $(Y_{1-c}Tb_c)_3Fe_5O_{12}$ and $(Y_{1-c}Yb_c)_3Fe_5O_{12}$ with $c\cong1.0$, 0.75, and 0.5. If $g$ does not change much with concentration, then from Eqs. (13) and (14) together with Eqs. (8) and (9), we expect $\Delta\omega/\omega$ to vary as $c^2$ and $Q_H^{-1}$ to vary as $c^3$. For YbIG at 78°K, $g$ is nearly constant as $c$ decreases, and we observe very nearly these dependences. In TbIG at room temperature, however, $g$ changes very much with concentration since the compensation point is at $\sim$250°K and moves lower rapidly as $c$ is decreased from unity, thus increasing $M_{\rm tot}$. This causes the concentration dependences to be in the range $c^4$ and $c^5$ for $\Delta\omega/\omega$ and $Q_H^{-1}$, respectively, for $1.0>c>0.5$. The agreement here with experiment is also quite good. These results for terbium and ytterbium concentration dependences lend additional support to the correctness of the field-dependent terms in Eqs. (13) and (14) as well as the form of $g$ in Eq. (25).

### D. Magnetoelastic Coupling Constants

$A_{\nu p}$ in Eq. (13) is a generalized magnetoelastic coupling constant. In the limit of $\omega\tau\rightarrow0$, which applies to the present acoustic measurements, $A_{\nu p}$ can be expressed in terms of the static magnetoelastic constants $B_1$ and $B_2$. In the lowest order in a cubic crystal there are two constants, $B_1$ and $B_2$, and they are defined by the relation for the magnetic energy density:

$$U_{\rm mag}=B_1(\alpha_x^2e_{xx}+\alpha_y^2e_{yy}+\alpha_z^2e_{zz})+B_2(\alpha_x\alpha_ye_{xy}+\alpha_y\alpha_ze_{yz}+\alpha_z\alpha_xe_{zx}), \tag{26}$$

where $\alpha_i$ are the direction cosines of the magnetization referred to the cubic axes, and $e_{ii}$ and $e_{ij}$ are the

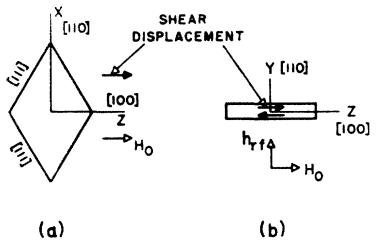


FIG. 6. Plan view (a) and edge view (b) of (110) disk. In (a), the $y$ axis is out of the page. The dc field $H_0$ and the shear displacement are along [100] in the plane of the disk. The rf driving (and detecting) field is along [110] perpendicular to the disk.

components of strain. In order to obtain a simple relation between $A_{\nu p}$ and $B_1$ and $B_2$, the disk geometry shown in Fig. 6 is much more advantageous than the spheres used previously. By holding the thin, diamond-shaped (110) disk at the corners, it is possible to make acoustic measurements with the applied dc field along a hard axis [100], as shown in the figure, in addition to the usual [111] axis, as in the case of spheres. Also both the shear and magnetization displacements are unidirectional. In Fig. 6 the applied rf magnetic field and the resulting rf magnetization are in the $y$ direction or perpendicular to the disk. Such rf magnetization can drive "thickness shear" modes with displacement directions lying almost anywhere in the plane of the disk. However, the mode for which $(\nu_\infty-\nu)$ is a maximum for a given value of $H_0$ is the "$e_{yz}$ mode," with shear displacement along the [100] axis as shown in Fig. 6(b). For this mode $A_{\nu\nu}{}^0$ in Eq. (13) is the elastic modulus $c_{44}$, and $A_{\nu p}$ and $A_{p\nu}$ are given by

$$(A_{\nu p})^2=(A_{p\nu})^2=g_{\mathrm{Fe}}\mu B_2^2/M_{\mathrm{Fe}}. \tag{27}$$

Thus, Eqs. (13) and (22) yield

$$B_2{}^2=\frac{g}{g_{\mathrm{Fe}}}2c_{44}M_{\mathrm{Fe}}(H_0+H_a+4\pi M_{\mathrm{tot}})\left(\frac{\nu_\infty-\nu}{\nu_\infty}\right)_{\max}^{[100]}, \tag{28}$$

where $4\pi M_{\mathrm{tot}}$ is a demagnetizing field. In high-temperature approximation, using Eq. (25), we obtain

$$B_2{}^2=2c_{44}M_{\mathrm{tot}}(H_0+H_a+4\pi M_{\mathrm{tot}})\left(\frac{\nu_\infty-\nu}{\nu_\infty}\right)_{\max}^{[100]}. \tag{29}$$

When the applied dc field is along the [110] axis, again in the plane of the disk, and the applied rf field is perpendicular to the disk as before, we obtain a similar relation for $B_1$, namely,

$$B_1{}^2=2c_{44}M_{\mathrm{tot}}(H_0+H_a+4\pi M_{\mathrm{tot}})\left(\frac{\nu_\infty-\nu}{\nu_\infty}\right)_{\max}^{[110]}. \tag{30}$$

When the dc field is along the [111] axis, $B_1$ and $B_2$ are mixed, and the mode with the maximum frequency shift yields the relation

$$\tfrac{1}{3}(2B_1{}^2+B_2{}^2)=2c_{44}M_{\mathrm{tot}}(H_0+H_a+4\pi M_{\mathrm{tot}})\left(\frac{\nu_\infty-\nu}{\nu_\infty}\right)_{\max}^{[111]}. \tag{31}$$

We can also estimate the contribution to the anisotropy field due to the macroscopic magnetostriction. Using $B_1$ and $B_2$ it is written

$$K_1(\text{mag. str.})=(1/2c_{44})(B_1{}^2-B_2{}^2). \tag{32}$$

We can see from the experimental values of $B_1$ and $B_2$ for TbIG and EuIG at room temperature, given below, that $K_1$(mag. str.) is an order of magnitude or more smaller than the observed static anisotropy constant.

Before giving the experimental results, a convenient relation to obtain $c_{44}$ for use in Eqs. (29)–(31) is given by

$$c_{44}=4\rho d^2\nu_\infty{}^2, \tag{33}$$

where $\rho$ is the density, $d$ is the thickness of the disk, and $\nu_\infty$ is the frequency of the mode with $\lambda/2$ across the thickness of the disk.

Experiments were performed at room temperature on approximately diamond-shaped (110) disks of TbIG and EuIG. They were 0.4 mm thick and approximately 6 mm on each edge. The shear modulus $c_{44}$ was found to be nearly the same as YIG in both cases, or approximately $7.7\times10^{11}$ dyn cm$^{-2}$. By curve fitting the data for $\nu$ vs $H_0$ to Eqs. (29) and (30) in the manner shown in Figs. 1 and 3, we obtained the results below. The data have given excellent fits to the equations in all cases. For TbIG, $|B_1|\leq3.5\times10^6$ erg cm$^{-3}$ and $|B_2|=30\times10^6$ erg cm$^{-3}$. For EuIG, $|B_1|=45\times10^6$ erg cm$^{-3}$ and $|B_2|\leq4.5\times10^6$ erg cm$^{-3}$.[12] The signs must still be determined from strain gauge measurements. We also obtained values of the anisotropy constant $K_1$. These are not as accurate as the $B$ values and are given only to show their consistency with observed static values, in the case of TbIG.[13] They are $K_1\cong6500$ erg cm$^{-3}$ for TbIG and 20,000 erg cm$^{-3}$ for EuIG. Measurements of $(\nu_\infty-\nu)/\nu_\infty$ have also been made with $H_0$ along [111], and the results were quite consistent with Eq. (31) and the above values of $B_1$ and $B_2$. The observed reversal of the magnetic anisotropy (ratio of $B_1$ to $B_2$) between TbIG and EuIG is being investigated as well as the temperature dependence of $B_1$ and $B_2$.

In connection with the latter point it may be noted that at lower temperatures Eq. (28) should be used rather than (29), together with the correct value of $g$. In heavily doped samples, $g$ is difficult to measure at low temperatures either by torque or resonance methods. However, it should be possible to obtain $g$ on heavily doped samples with the acoustic technique described here, using the relation

$$g=2g_{\mathrm{Fe}}K_1/H_aM_{\mathrm{Fe}}. \tag{34}$$

$H_a$ can be obtained by fitting $\nu$ vs $H_0$ to Eq. (28), and

[12] Professor S. Iida at Bell Telephone Laboratories has obtained, using strain gauges, a $B_1$ and $B_2$ for EuIG at room temperature of $-50\times10^6$ and $-4.2\times10^6$ erg cm$^{-3}$, respectively. The observed magnetoelastic constants for TbIG and EuIG may be compared with $|B_2|$ for YIG at room temperature of $7.4\times10^6$ erg cm$^{-3}$ obtained from acoustic wave rotation measurements, H. Matthews and R. C. LeCraw, Phys. Rev. Letters **8**, 397 (1962).

[13] R. F. Pearson, Suppl. J. Appl. Phys. **33**, 1236 (1962).

$K_1$ can probably be extrapolated from lightly doped samples. Thus $B_1$ and $B_2$, as well as $g$, may be obtained at low temperatures with the theory and techniques we have described.

Mention should be made of the low-temperature nature of the generalized magnetoelastic constant $A_{\nu p}$. In general, $A_{\xi\eta}$ is given by Eq. (19). The second term of Eq. (19) becomes very large when the temperature is lower than the lowest excited level and the lowest excited level is very small. This phenomenon has been observed as a giant anisotropy in the case of $A_{pp}$.[10] It is expected that the same thing should happen also to $A_{\nu p}$, or in the magnetoelastic coupling constants. At high temperatures, Eq. (21) is applicable and such a "giant" effect disappears.

Here we have treated the case of the low-frequency limit. When the frequency becomes higher, the frequency-dependent character of $A_{\xi\eta}$ becomes important. Such a phenomenon occurs in spin resonance experiments, treated in paper II, where the frequency is more than three orders of magnitude larger than in the acoustic experiments described herein.

## ACKNOWLEDGMENTS

We wish to express our appreciation to J. P. Remeika for his continued assistance to this work by his growth of the crystals and other discussions, and also to S. Iida for communicating the results of his strain gauge measurements of $B_1$ and $B_2$ on EuIG, and for a number of useful discussions on magnetoelastic phenomena. We also wish to thank C. Herring for his critical reading of the manuscript and for helpful discussions.

## APPENDIX I

When the driving forces are given by $f_q \cos\omega t$ and $f_\nu \cos\omega t$, the equation of motion for $S_p$ and $\Delta_\nu$ are given by

$$(\pm)\hbar dS_p/dt = F_q + f_q \cos\omega t, \tag{1.1}$$

$$-(\hbar^2/K_\nu)d^2\Delta_\nu/dt^2 = F_\nu + f_\nu \cos\omega t, \tag{1.2}$$

where $p=x$ or $y$ and $(\pm)$ corresponds to $(x,y)$. Because these are linear equations, and we are interested in the stationary solution, we can treat these by the usual complex number method. That is, the driving force is written as $f_\xi e^{i\omega t}$ and $\Delta_\xi$ as $\Delta_\xi^0 e^{i\omega t}$, where $\Delta_\xi^0$ is a complex number, and the real solution is given by the real or imaginary part of it, namely $\mathrm{Re}[\Delta_\xi^0 e^{i\omega t}]$. Then Eqs. (1.1) and (1.2) are written as

$$\sum T_{\xi\eta}\Delta_\eta^0 = -f_\xi \tag{1.3}$$

where

$$T_{\xi\eta} = T_{\xi\eta}{}^r + iT_{\xi\eta}{}^i, \tag{1.4}$$

$$T_{\xi\eta}{}^r = A_{\xi\eta} - (\hbar^2\omega^2/K_\nu)\delta_{\xi\nu}\delta_{\eta\nu}, \tag{1.5}$$

$$T_{\xi\eta}{}^i = a_{\xi\eta} + \hbar\omega(\delta_{\xi x}\delta_{\eta y} - \delta_{\xi y}\delta_{\eta x}). \tag{1.6}$$

Then $\Delta_\eta^0$ is solved as

$$\Delta_\eta = |T^{\eta f}|/|T|, \tag{1.7}$$

where $|T|$ is the determinant of $T_{\xi\eta}$ and $|T^{\eta f}|$ is the determinant where the $\eta$ column is substituted by $f_\xi$.

We assume now that the damping terms, namely, $a_{\xi\eta}$, are much smaller than the real terms, namely, $A_{\xi\eta}$; and we take into account only the lowest order terms with respect to the damping terms. In such a case, the resonance frequencies are determined only postulating that the real part of $|T|$ is zero, and the linewidths are determined from the imaginary part of $|T|$. The real part is written as

$$\begin{aligned}(A_{\nu\nu}-\hbar^2\omega^2/K_\nu)(A_{\mu\mu}-\hbar^2\omega^2/K_\mu)[&(A_{xx}A_{yy}-A_{xy}A_{yx}\\ &-\hbar^2\omega^2)+\sum_{\xi=\nu,\mu}(A_{x\xi}A_{\xi y}A_{yx}+A_{y\xi}A_{\xi x}A_{xy}\\ &-A_{x\xi}A_{\xi x}A_{yy}-A_{y\xi}A_{\xi y}A_{xx})/(A_{\xi\xi}-\hbar^2\omega^2/K_\xi)\\ &+(A_{\nu x}A_{\mu y}-A_{\mu x}A_{\nu y})(A_{x\nu}A_{y\mu}-A_{x\mu}A_{y\nu})/\\ &(A_{\nu\nu}-\hbar^2\omega^2/K_\nu)(A_{\mu\mu}-\hbar^2\omega^2/K_\mu)],\end{aligned} \tag{1.8}$$

where we have considered that only an acoustic phonon, $\nu$, an optical phonon, $\mu$, and an acoustic magnon with $x$ and $y$ components are coupled strongly with each other. Postulating Eq. (1.8) equals zero, we obtain three solutions of $\omega$. In the following, we assume for simplicity that $A_{xy}=A_{yx}=0$, and $A_{\xi\eta}=A_{\eta\xi}$. The first assumption implies that there exists an interaction only by the magnetoacoustic coupling. The second implies the symmetry relation of $A_{\xi\eta}$.

(*i*) *Acoustic mode, $\nu$:* We consider here the case where the Zeeman frequency is much higher than the acoustic frequency. Then the following relations exist

$$A_{xx}A_{yy} \gg \hbar^2\omega_a^2, \quad A_{\mu\mu}K_\mu \gg \hbar^2\omega_a^2. \tag{1.9}$$

Then the frequency of the acoustic mode is given by

$$\hbar^2\omega_a^2 = A_{\nu\nu}K_\nu - K_\nu\left[\frac{A_{xx}A_{y\nu}^2+A_{yy}A_{x\nu}^2-(A_{\nu x}A_{\mu y}-A_{\mu x}A_{\nu y})^2/A_{\mu\mu}}{A_{xx}A_{yy}-(A_{xx}A_{y\mu}^2+A_{yy}A_{y\mu}^2)/A_{\mu\mu}}\right]. \tag{1.10}$$

(*ii*) *Optical mode, $\mu$:* Now instead of Eq. (1.9), the following exists:

$$A_{xx}A_{yy} \ll \hbar^2\omega_{\mathrm{op}}^2, \quad A_{\nu\nu}K_\nu \ll \hbar^2\omega_{\mathrm{op}}^2. \tag{1.11}$$

Therefore, $\omega_{\mathrm{op}}$ is given approximately as

$$\hbar^2\omega_{\mathrm{op}}^2 = A_{\mu\mu}K_\mu + (A_{xx}A_{y\mu}^2+A_{yy}A_{x\mu}^2)/A_{\mu\mu}. \tag{1.12}$$

Usually the second term is negligible.

(*iii*) *Magnetic mode:* The resonant frequency is given by

$$\hbar^2\omega^2 = A_{xx}A_{yy} - \sum_\xi \frac{A_{xx}A_{y\xi}^2+A_{yy}A_{y\xi}^2}{A_{\xi\xi}-\hbar^2\omega^2/K_\xi} - \frac{(A_{x\nu}A_{y\mu}-A_{x\mu}A_{y\nu})^2}{(A_{\nu\nu}-\hbar^2\omega^2/K_\nu)(A_{\mu\mu}-\hbar^2\omega^2/K_\mu)}. \tag{1.13}$$

In the present case, the following relation exists

$$A_{\nu\nu}K_\nu \ll \hbar^2\omega^2 \ll A_{\mu\mu}K_\mu. \tag{1.14}$$

Then Eq. (1.13) is approximated by

$$\hbar^2\omega^2 = A_{xx}A_{yy} - (A_{xx}A_{y\mu}{}^2 + A_{yy}A_{x\mu}{}^2)/A_{\mu\mu}. \tag{1.15}$$

The physical meaning of the equations is clear. The optical frequency is so high that the acoustic mode can not follow it. Therefore, $(\hbar\omega_{\rm op})^2$ is simply given by $A_{\mu\mu}K_\mu$. The frequency of the long-wavelength acoustic spin mode is between those of the long-wavelength acoustic and optical lattice vibrations, and so only the optical vibration follows it. This is given by Eq. (1.15), and the second term is the anisotropy due to the optical magnetostriction effect. The frequency of the acoustic lattice vibration is lowest, so the other two modes can follow it. But the main effect of the optical lattice vibration appears only through the spin-wave mode. In other words, the effect of the optical mode is already included when we use the spin-wave mode modified by the optical mode as given in Eq. (1.15) because the direct interaction between the acoustic and optical vibrations are neglected in the present treatment. Usually the last term of Eq. (1.15) is not a main term because of the large term $A_{\mu\mu}$, and in Eqs. (10) and (13), of paper I, this term is dropped for simplicity. Or, in another approach, it is possible to consider that all optical modes are included in the individual modes part, $\mathcal{H}_0$, in Eq. (1), and then not to treat the $\mu$ mode particularly.

The imaginary part of $|T|$ is written as

$$\begin{aligned}(A_{\nu\nu}-\hbar^2\omega^2/K_\nu)(A_{\mu\mu}-\hbar^2\omega^2/K_\mu)[a_{xx}A_{yy}+a_{yy}A_{xx}\\ +\sum_{\xi=\nu,\mu}\{a_{\xi\xi}(A_{xx}A_{yy}-\hbar^2\omega^2)-2a_{x\xi}A_{x\xi}A_{yy}\\ -2a_{y\xi}A_{y\xi}A_{xx}-a_{xx}A_{y\xi}{}^2-a_{yy}A_{x\xi}{}^2\}/\\ (A_{\xi\xi}-\hbar^2\omega^2/K_\xi)],\end{aligned} \tag{1.16}$$

where again the following relations were used, namely, $A_{xy}=A_{yx}=0$, $A_{\xi\eta}=A_{\eta\xi}$, and the same for the $a_{\xi\eta}$ terms. Also higher order terms with respect to $(A_{\nu\nu}-\hbar^2\omega^2/K_\nu)^{-1}$, etc., have been omitted.

The usual linewidth $\Delta\omega$ is defined as $2|\omega_0-\omega_{1/2}|$, where $\omega_{1/2}$ is the frequency corresponding to half the maximum absorption. Or, $\omega_{1/2}$ corresponds to the frequency where the real and imaginary parts of $|T|$ are equal. Therefore, $\Delta\omega$ is given by dividing Eq. (1.16) by $\frac{1}{2}d|T|/d\omega$. On the other hand, the inverse relaxation time of the energy, $\tau^{-1}$, is given by the imaginary part of $\omega$ in a freely decaying mode. Therefore, when the damping is small, it is clear that $\Delta\omega=\tau^{-1}$.

(*i*) *Magnetic mode:* Using Eqs. (1.14) and (1.15), Eq. (1.16) is written as

$$\begin{aligned}(A_{\nu\nu}-\hbar^2\omega^2/K_\nu)[a_{xx}(A_{\mu\mu}A_{yy}-A_{y\mu}{}^2)+a_{yy}(A_{\mu\mu}A_{xx}-A_{x\mu}{}^2)\\ -2a_{x\mu}A_{x\mu}A_{yy}-2a_{y\mu}A_{y\mu}A_{xx}\\ +a_{\mu\mu}(A_{xx}A_{y\mu}{}^2+A_{yy}A_{x\mu}{}^2)/A_{\mu\mu}].\end{aligned} \tag{1.17}$$

On the other hand, $\frac{1}{2}d|T|/d\omega$ is a very complicated function because of the frequency-dependent character of $A_{\xi\eta}$. If we neglect the frequency dependence of $A_{\xi\eta}$, we obtain the following result

$$\tfrac{1}{2}d|T|/d\omega = (A_{\nu\nu}-\hbar^2\omega^2/K_\nu)A_{\mu\mu}\hbar^2\omega. \tag{1.18}$$

For the case in this paper, however, the frequency dependence of $A_{\xi\eta}$ is not negligible. Experimentally, $\Delta H$ is usually measured, not $\Delta\omega$. To get $\Delta H$, Eq. (1.16) is divided by $\frac{1}{2}d|T|/dH_0$. Again $A_{\xi\eta}$ also depends on $H_0$, but since the exchange field is usually much larger than the external field, we can neglect in the zeroth approximation the field dependence of $A_{\xi\eta}$, except for $A_{xx}$ and $A_{yy}$. $A_{pp}$ is then written as

$$A_{pp}=A_{pp0}+(\partial A_{pp}/\partial H_0)H_0 \equiv g_p\mu(H_0+H_{pa}). \tag{1.19}$$

Then $\frac{1}{2}d|T|/dH_0$ is given as

$$\begin{aligned}\tfrac{1}{2}d|T|/dH_0 = \tfrac{1}{2}(A_{\nu\nu}-\hbar^2\omega^2/K_\nu)[(A_{\mu\mu}A_{xx}-A_{x\mu}{}^2)g_y\\ +(A_{\mu\mu}A_{yy}-A_{y\mu}{}^2)g_x].\end{aligned} \tag{1.20}$$

Note that even in the special case given in Eq. (1.18) $\hbar\Delta\omega$ and $g\mu\Delta H$ are the same only when the $x$ and $y$ components are equivalent and the anisotropy due to local magnetostriction is small. Also Eq. (12) is obtained by the same assumption as above, namely, omitting the last three terms in Eq. (1.17).

(*ii*) *Acoustic mode, $\nu$:* Using Eqs. (1.9) and (1.10), (1.16) is written as

$$\begin{aligned}A_{\mu\mu}[A_{xx}A_{yy}a_{\nu\nu}+(A_{yy}/A_{xx})A_{x\nu}{}^2a_{xx}+(A_{xx}/A_{yy})A_{y\nu}{}^2a_{yy}\\ -2A_{x\nu}A_{yy}a_{x\nu}-2A_{y\nu}A_{xx}a_{y\nu}],\end{aligned} \tag{1.21}$$

where for simplicity we have neglected local magnetostriction effects.

Concerning the derivative of $|T|$ with respect to $\omega$, the frequency dependence of $A_{\xi\eta}$ is neglected because the frequency of the long-wavelength acoustic mode is sufficiently low. Then we get,

$$\tfrac{1}{2}d|T|/d\omega = A_{\mu\mu}A_{\nu\nu}A_{xx}A_{yy}/\omega_a \tag{1.22}$$

and thus Eq. (14) is obtained.